Ab initio calculations of electron affinity and ionization potential of carbon nanotubes

F Buonocore[1], F Trani[2], D Ninno[2], A Di Matteo[3], G Cantele[4] and G Iadonisi[4]

[1] STMicroelectronics, Stradale Primosole 50, 95121 Catania, Italy
[2] Coherentia CNR-INFM, INFN Sezione di Napoli and Università di Napoli "Federico II", Dipartimento di Scienze Fisiche, Complesso Universitario Monte S. Angelo, Via Cintia, I-80126 Napoli, Italy.
[3] STMicroelectronics c/o IMAST P.le Enrico Fermi 1, Località Granatello Portici I-80055 Naples, Italy
[4] Coherentia CNR-INFM and Università di Napoli "Federico II", Dipartimento di Scienze Fisiche, Complesso Universitario Monte S. Angelo, Via Cintia, I-80126 Napoli, Italy.

Abstract. Combining ab initio all-electron and plane wave pseudopotential calculations we have studied the electron affinity (EA) and the ionization potential (IP) of (5,5) and (7,0) single wall carbon nanotubes. The role played by finite size effects and nanotube termination have been analyzed comparing hydrogen passivated and no passivated nanotubes of different lengths. We show that the EA and the IP are determined by the interplay between the quantum confinement due to the nanotube finite length and the charge accumulation on the edges due to its finiteness. The band structure, EA and IP of carbon nanotube arrays have also been studied. We show that in this case the EA and the IP are also controlled by the array density.

PACS numbers: 81.07.De, 31.15.Ar, 73.20.At

E-mail: `francesco.buonocore@st.com`

Submitted to: *Nanotechnology*

1. Introduction

Interfacing carbon nanotubes either with a metal or with a semiconductor is certainly a most important step in the development of nanoscale electronic devices [1]. Apart from certain important aspects related to the formation of dipoles at the interface, it is well known that the electronic structure alignment of the two materials near the Fermi level is largely determined by the mismatch between the Fermi level of the substrate and the electron affinity/ionization potential of the adsorbed material. These are the driving concepts in the design of rectifiers, p-n junctions and transistors [1].

The vast majority of published theoretical works concerning a nanotube surface property are concentrated on ab initio calculations of the work function (WF). The dependence of the WF on size, chirality and orientation [2, 3, 4, 5] has been studied. Bundles of nanotubes have also been considered [4, 6]. Apart from differences due to different ways of defining the work function and to different computational schemes, the general trend coming from these papers is that, with the exception of small diameter tubes, the work function does not dramatically vary upon changing the tube chirality [2] and capping [3]. Strangely enough, the electron affinity (EA) and the ionization potential (IP), although related to WF, have not received much attention, neither it has been discussed the interplay between these quantities and the presence of edge localized states. It is expected that these states may play an important role in interfacing a carbon nanotube with another material.

The field emission also depends on the EA and IP. In particular, the high aspect ratio (height to diameter) of carbon nanotubes makes them an interesting material for realizing low threshold voltage field emitters. These types of devices include lamps, x-ray tubes and flat panel display. A rich literature has been flourishing in the last years on the field emission effect. It is important to note that although early studies reported field emission where the carbon nanotubes were dispersed in the substrate [7], more recent works achieved an excellent vertical alignment with homogeneous length and radius [8]. Moreover, the development of nanopatterning techniques for catalyst deposition, is, in our opinion, opening the way toward the fabrication of nanotubes arrays with a predefined geometry and an intertube distance on the nanometer scale length. As we shall see in the following, when the intertube distance is of the order few Å, the interactions between the nanotubes give rise to a band structure whose main features depend on the nanotube nature (chirality, either open or close edges and so on).

Motivated from the above considerations, in this paper we investigate the electronic properties of single wall carbon nanotubes with methods rooted on the Density Functional Theory. We have analyzed two classes of systems: the isolated nanotube and the corresponding periodic array. In the first case the emphasis is on the dependence of EA and IP on both the nanotube type, either armchair or zig-zag, and length. In the second case we have analyzed the array band structure and the variations of EA and IP with the intertube distance. In both the cases, some indications are given on the

corresponding work function variations.

2. Computational details

The ab initio calculations have been performed using two different computational schemes. The first one is an all-electron method as implemented into the DMol^3 package (Accelrys Inc.) [9, 10] which uses a localized basis set. As such, the package is particularly useful in studying confined and isolated systems. The second one is based on a pseudopotential plane wave method as implemented in the QUANTUM-ESPRESSO code [11]. This code is a good choice for periodic systems such as the nanotube arrays. Our past experience in using such mixed computational schemes is that, provided the same exchange and correlation functional is used, the numerical convergence has been reached and a sufficiently large supercell is implemented for the plane wave code, the two methods give results in good agreement [12].

All the calculations have been done using the generalized gradient approximation (GGA) with the Perdew, Burke and Ernzerhof (PBE) [13] correlation functional. For the all-electron calculations the electronic wave functions are expanded in atom-centered basis functions defined on a dense numerical grid. The chosen basis set was the Double Numerical plus polarization [14]. This basis is composed of two numerical functions per valence orbital, supplemented with a polarization function, including, where necessary, a polarization p-function on all the hydrogen atoms. The pseudopotential plane wave calculations have been performed using ultrasoft pseudopotentials, a 26 Rydberg cut-off for the wavefunctions and a 156 Rydberg cut-off for the charge density. Since the nanotubes considered for the array calculations have a finite length of 8.15 Å, we have used a supercell whose dimension along the nanotube axis has been fixed at 20 Å. We have checked that this supercell height is sufficient to avoid spurious interactions between the array periodic replicas. We have also verified that a 2×2 k-point grid is enough for having converged total energies and band structures. For both the calculation schemes, we used a convergence threshold on the force for the geometry optimizations of 0.001 Ry/Å.

3. Results and discussion

3.1. Isolated Nanotubes

As mentioned before, we have investigated the electronic structure of isolated nanotube with all-electron calculations. We have focused our attention on two different types of nanotubes: zig-zag (7,0) and armchair (5,5) nanotubes of different lengths. In both the cases, we have taken the nanotube edges either passivated with hydrogens (H-pass) or allowed the edge carbon atoms to relax without constrictions (no-pass).

In Fig.1 we plot the electronic orbitals of the H-pass (7,0) nanotube whose energies are around the HOMO (Highest Occupied Molecular Orbital) and the LUMO (Lowest Unoccupied Molecular Orbital). In these calculations the nanotube length has been fixed

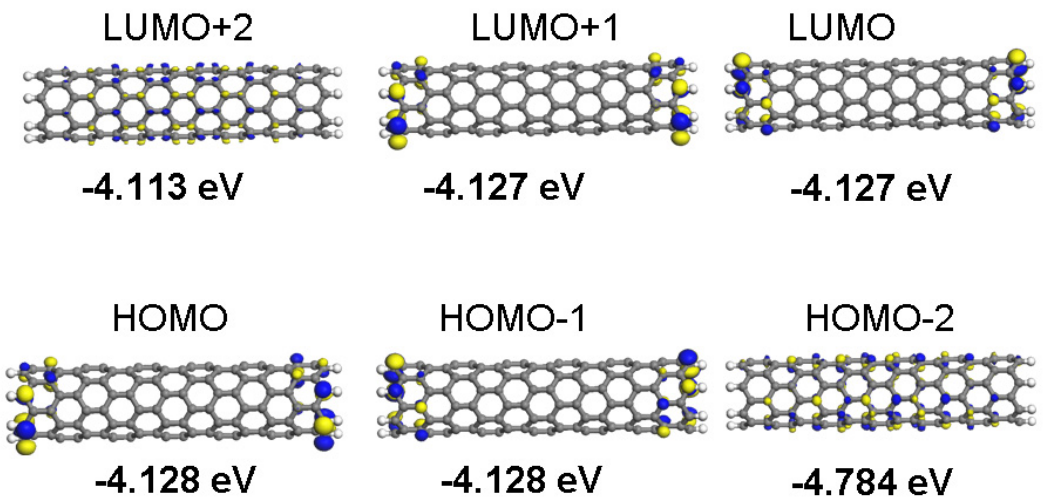

Figure 1. (Color online) Molecular orbitals and energy levels of H passivated open edge (7,0) carbon nanotube.

to 23.9 Å. It can be seen from this figure that there are four edge localized orbitals, two HOMOs and two LUMOs which are basically degenerate. The H-pass (5,5), not shown in the figure, has no edge localized orbitals. It is worth mentioning that these results are consistent with those of H-pass graphene ribbons. Indeed, in Ref.[15] an analytic expression for the electronic wave functions of the edge states for graphene ribbons has been derived in the case of zigzag edges. It has been shown that the nature of this edge states is topological and, indeed, they were not predicted for armchair structures, in agreement with our findings. As one would expect, the pattern of the edge states changes completely when the passivating hydrogens are removed. In this case the orbitals of both the (5,5) and (7,0) nanotubes exhibit edge localized states mainly due to the presence of dangling bonds. We have found that the no-pass (5,5) nanotube shows delocalized HOMO and LUMO orbitals, together with four edge localized orbitals very near in energy, lying at 0.285 eV above the LUMO delocalized orbital. The no-pass (7,0), on the other hand, has a richer number of localized orbitals, four localized orbitals above and two localized orbitals below the HOMO level. We shall see in the following that this complex interplay between edge localized and delocalized orbitals has some influence on both the EA and IP, and, in the case of a nanotube array, on the band structure.

In Fig.2 we plot the total Mulliken charge computed on atomic planes perpendicular to the nanotube axis. Because of symmetry, the plot is limited to half the distance from the nanotube edges. These calculations have been done taking, for each case, nanotubes with two different lengths. The first observation to be made is that the Mulliken charge near the nanotube edge has only a very weak dependence on the nanotube length. The second point is that there are significant differences depending on the nanotube type and the edge termination. The (5,5) H-pass has a dipole near the edge reflecting the ability of the hydrogen atom to donate its electron. Because of the armchair shape, the edge carbon atoms tend to form a double bond. In the (5,5) no-pass this dipole is reversed and this is because some electronic charges migrate from the nanotube to the edge. At the same time, the armchair carbon atoms give rise to triple bonds. A good indication toward this interpretation comes from the calculation of the carbon-carbon bond lengths on the nanotube edge. For the H-pass nanotube we have found a carbon-carbon distance of 1.37 Å to be compare with the double bond of C_2H_4 which we have calculated to be 1.33 Å. For the no-pass nanotube the bond length has been of 1.24 Å to be compared with that of the triple bond of C_2H_2 which was 1.20 Å. In all the other cases, including the no-pass (7,0) nanotube, the carbon-carbon bond length is in the range 1.42÷1.44 Å being similar to that of graphene. Fig.2 shows that the (7,0) nanotube has a different behavior in the sense that there is no dipole flipping on the edge. This is due to the zig-zag shape of the edge which tend to preserve the graphene bonding pattern. In any case, it should be noted that the removal of the hydrogens from the edge does induce a redistribution of charge in the first couple of atomic planes.

For giving a more detailed account of the effects induced by the charge distribution highlighted by the Mulliken analysis of Fig.2, we show in Fig.3 a 2D contour plot of the all-electron electrostatic potential calculated for a (5,5) nanotube considering both the H-pass and the no-pass edges. At large distance from the nanotube, this potential defines the vacuum level so that its distribution around the nanotube cage gives the local variations of the work function. The large difference between the two cases is very evident. In the H-pass nanotube (panel a) the potential raises very rapidly in the direction orthogonal to the nanotube axis while for the no-pass case the growth is rapid on the edges. Another interesting feature is the potential distribution inside the nanotube cage. The hydrogen passivation lowers the potential on the edges whereas the bonding between carbon atoms that occurs when the hydrogens are removed lowers the potential inside the cage. This findings are fully consistent with the charge distributions given in Fig.2.

The electron affinity is usually defined as $EA = E(N+1) - E(N)$ where $E(N)$ and $E(N+1)$ are the total ground-state energies in the neutral (N) and singly charged $(N+1)$ configurations. In a similar way, the ionization potential is defined as $IP = E(N-1) - E(N)$. Although this definition may be very useful for systems such as molecules and small nanocrystals, it is better to change it in extended systems because in this case those energy differences are dominated by band structure terms. Once the vacuum level E_{vac} has been determined, EA and IP can be defined starting

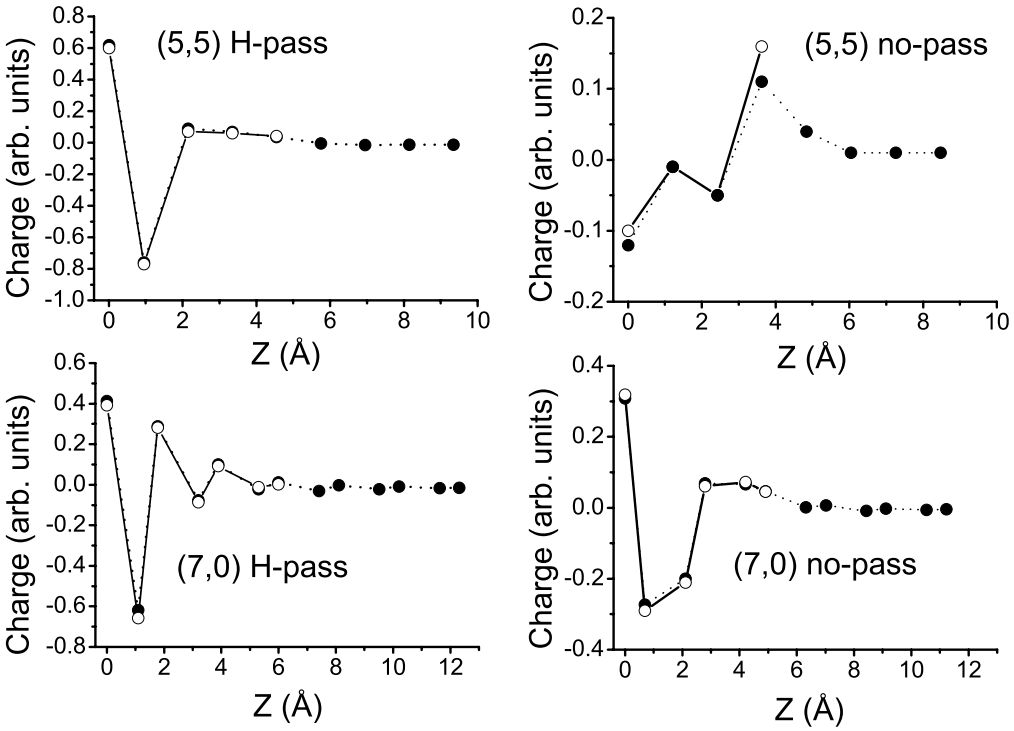

Figure 2. Total Mulliken charge calculated on planes perpendicular to the nanotube axis. For each nanotube type, the calculation have been done for two different lengths corresponding to full and open circles.

from the LUMO and HOMO states as $EA = E_{vac} - E_{LUMO}$ and $IP = E_{vac} - E_{HOMO}$. Assuming a Fermi level sitting in the middle of the gap, the work function is simply given by $WF = (EA + IP)/2$. Although our finite and isolated carbon nanotubes can be considered as a large molecule, we have preferred to define EA and IP in terms of LUMO and HOMO states since this choice is consistent with the case of a nanotube array which will be discussed in the next section. We have seen above that there may be cases in which the LUMO and the HOMO can either be localized on the nanotube edges or may be extended over all the structure. It is therefore worth showing what the EA and IP would be when referred to both these states. This will be done for the (7,0) nanotube.

The periodic (5,5) nanotube is a zero gap metal for which we have obtained an all-electron WF of 4.37 eV. The plane wave calculation gives 4.28 eV. For the periodic (7,0) nanotube we have an all-electron WF of 4.82 eV to be compared with the plane wave result of 4.75 eV. Although in both the case the two methods are in good agreement, it should be mentioned that our calculated work functions for the infinite nanotube are smaller than that of ref. [2]. It is possible that the deviations are due

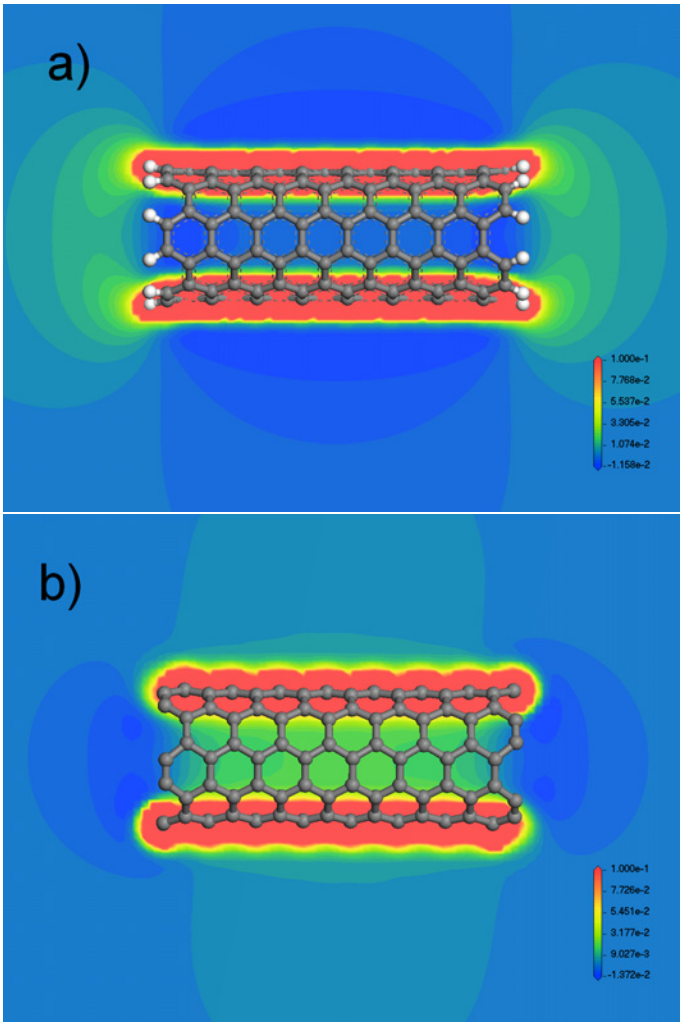

Figure 3. (Color online) Planar contour plots of the all-electron electrostatic potential of a (5,5) carbon nanotube with (panel a)) and without (panel b)) hydrogen atoms on the nanotube open edge. The legend is in atomic units and negative values correspond to higher potential.

to the difference between LDA and GGA exchange and correlation functionals. In any case, the comparison with the many experimental data available is acceptable. TEM measurements on multiwall nanotubes give 4.6-4.8 eV [16], photoelectron emission gives 4.95 eV and 5.05 eV for multi- and single wall [17], thermionic emission for multi-wall gives 4.54-4.64 eV [18], UPS measurements on single wall gives 4.8 eV [19].

In a finite nanotube, quantum confinement may give a strong dependence of the electronic properties on the nanotube length. To give a clear insight on this effects, we have calculated the EA and IP for a number of tubes with increasing length. The results are shown in Fig.4 where we show the calculated EA and IP of a (5,5) nanotube with the edges passivated with hydrogens. Both EA and IP, as well as the gap, exhibit regular oscillation on increasing the nanotube length. Despite of this, the quantum confinement

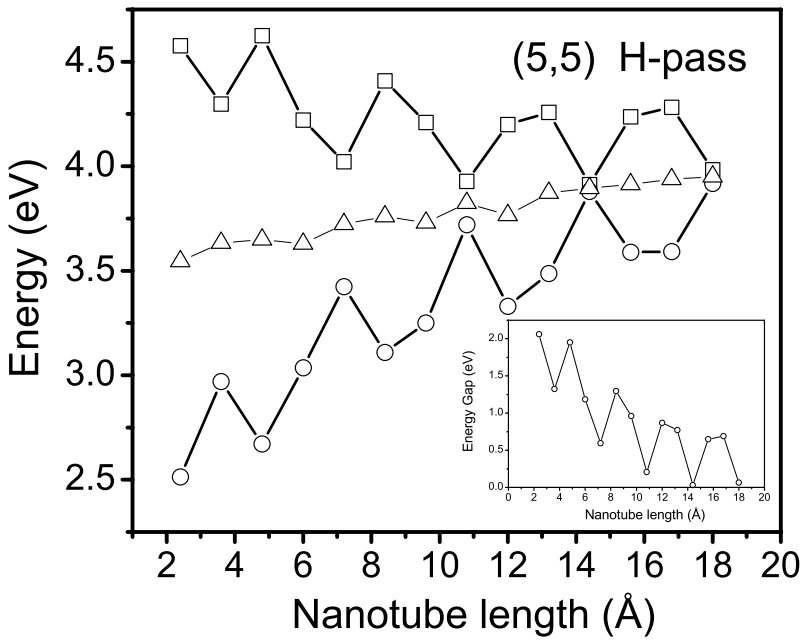

Figure 4. Ionization potential (squares), electron affinity (circles) and work function (triangles) of a H-pass (5,5) nanotube as a function of its length. The inset shows the evolution of the energy gap with the nanotube length.

effects is evidenced by the fact that EA and IP tend, for long nanotube, to approach each other. This tendency toward metallicity is even more evident looking at the evolution of the energy gap shown in the inset of Fig.4. The nature of the oscillating energy gaps has been discussed in Ref.[20], where it is shown, with a tight binding calculation, that inserting the quantum box boundary conditions in the band gap equation determined by the linear dispersion near the Fermi k-point, the gap of the finite armchair nanotube is found to vanish every 3 sections (see Ref. [20] for the definition of a section). Our calculations shows that the energy gap does not vanish completely and this is because the interactions go well beyond the first few nearest-neighbors. An interesting aspect of the results shown in Fig.4 is that the work function, defined as $WF = (EA + IP)/2$, is not influenced by these strong oscillations. Over the explored range of nanotube lengths, WF has an overall variation of about 0.5-0.6 eV. As far as the no-pass (5,5) is concerned, we have found a similar dependence on the nanotube length of both EA and IP. However, because of the flipping of the nanotube edge dipoles shown in Fig.2, EA, IP and therefore the work function are raised in energy. For instance, for the longest nanotube shown in Fig.4, we have found that EA and IP are raised of 0.6 eV with respect to those of H-pass nanotubes.

In Fig.5 we show the IP and EA defined either with respect to delocalized HOMO and LUMO (dash joining line) or with respect to the edge localized ones (full joining

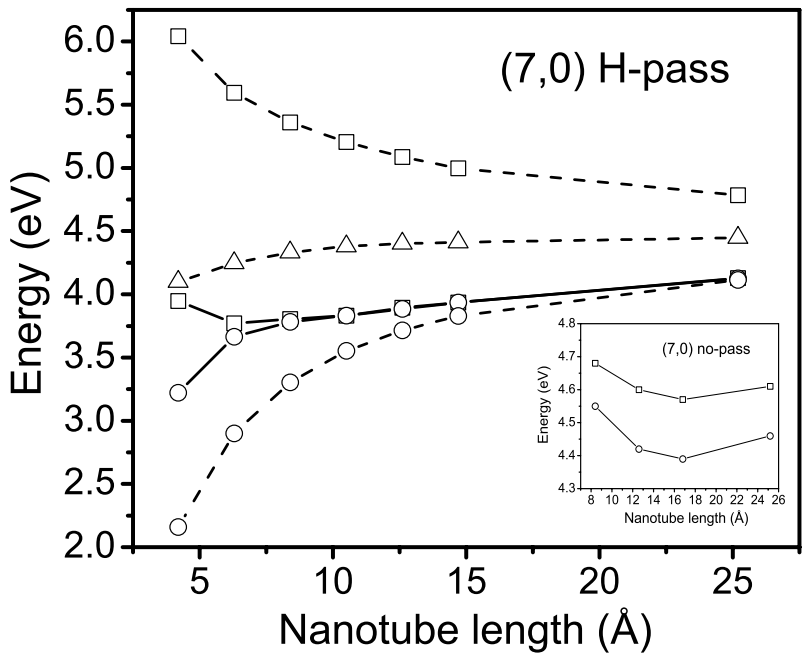

Figure 5. Ionization potential (squares), electron affinity (circles) and work function (triangles) of (7,0) nanotube as a function of the nanotube length. The full joining line are referred to edge localized states whereas the dash joining lines are for data obtained from delocalized states. In the inset the results for the no passivated (7,0) are shown.

line) for a (7,0) H-pass nanotube. In the same figure we draw the WF obtained from the delocalized HOMO and LUMO. The first point to be noticed in Fig.5 is the clear quantum confinement effect on IP and EA when referred to delocalized orbitals. However, the work function has a weaker dependence on the nanotube length with an overall variation, for the length range considered, of about 0.4-0.5 eV. The HOMO and LUMO edge localized orbitals get approaching each other becoming almost degenerate with the delocalized HOMO. The inset of Fig.5 shows the results for the no-pass nanotube. Since both the HOMO ad the LUMO are localized on the edges, the dependence on the nanotube length is very weak.

3.2. Nanotube Arrays

We have studied (5,5) nanotube arrays using the QUANTUM-ESPRESSO [11] code. The nanotubes, whose length have been fixed at 8.15 Å, are organized in such a way to compose a 2D square lattice. When constructing the array, the first decision one has to make is on how to take the relative orientation of the nanotubes. This is an interesting point whose assessment requires an accurate description of the long-ranged

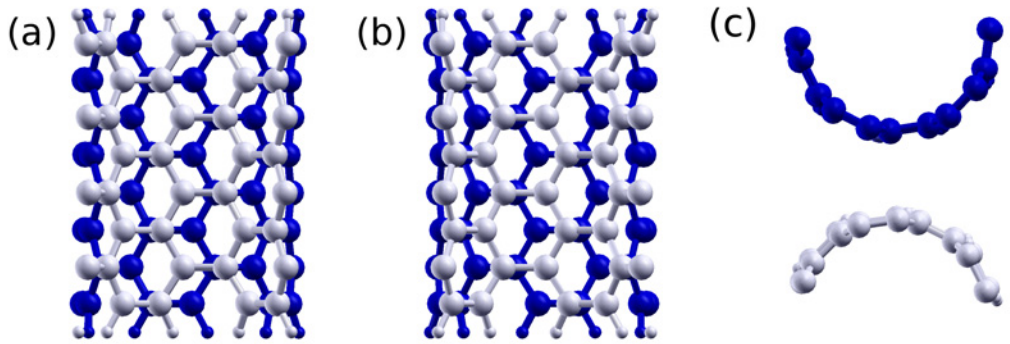

Figure 6. (Color online) Views along a) x, b) y and c) z of two adjacent nanotubes constituting the array.

(van der Waals) interaction between nanotubes. In a recent paper [21] the modelling of the intertube interaction has been studied within a tight binding scheme showing that two adjacent and parallel nanotubes have a minimum energy when are rotated in such way to have a stacking similar to that of graphite. Unfortunately, for reproducing such a stacking in our DFT calculations it would be necessary to use very large supercells making the calculation unpractical. Nevertheless, we have made a series of total energy calculations rotating, around its axis, just one nanotube in the unit cell. Although the long range intertube interactions are not well represented in our GGA calculations, we have found a minimum in the total energy when the nanotubes have a stacking very near to that of ref. [21]. The result is shown in Fig.6 through three views of two adjacent nanotubes. The similarity to the graphite stacking is evident.

In Fig.7 the square array band structures of H-pass (left panel) and no-pass (right panel) are shown. The lattice constant has been fixed at $a = 10$ Å that corresponds to a wall-wall distance of 3.2 Å. The usual notation of the reciprocal square lattice irreducible wedge has been used with the top valence band chosen as the zero energy. An interesting result coming from Fig.7 is that the top valence band is practically independent of the nanotube edge passivation. The bottom conduction band is instead dispersionless and, contrary to the valence band, it has a significant dependence on whether or not the nanotube edges are terminated with hydrogens. In particular, the number of conduction bands near the energy gap increases in the no-pass nanotube because of the presence of dangling bonds. It should also be noted that the fundamental energy gap occurs at the M point of the irreducible wedge.

In Fig.8 the EA, IP and WF of no-pass (panel a) and H-pass (panel b) nanotube arrays are shown as a function of the array lattice parameter. Interesting differences between the no-pass and the H-pass nanotube arrays arise. Indeed, from Fig.8 it can be noted that the EA and IP are greater than the isolated nanotube in the no-pass case while they are smaller in the H-pass case. The trend shown in Fig.8 can be easily discussed in terms of nanotube edge dipoles. As we have seen with the all-electron calculation in section 3.1, there is some charge accumulation near the nanotube

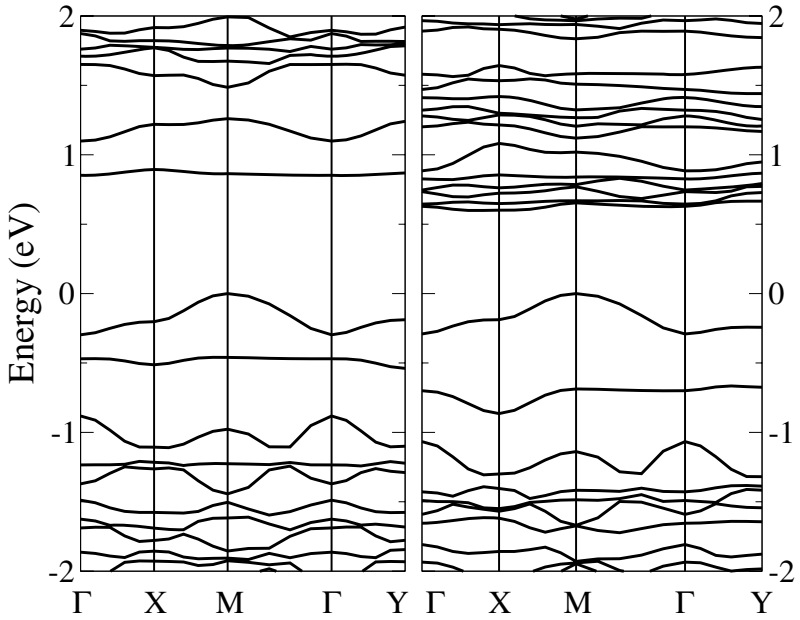

Figure 7. Band structures of H-pass (left) and no-pass (right) (5,5) nanotube arrays. The nanotubes have a length of 8.15 Å while the array has a lattice constant of 10 Å

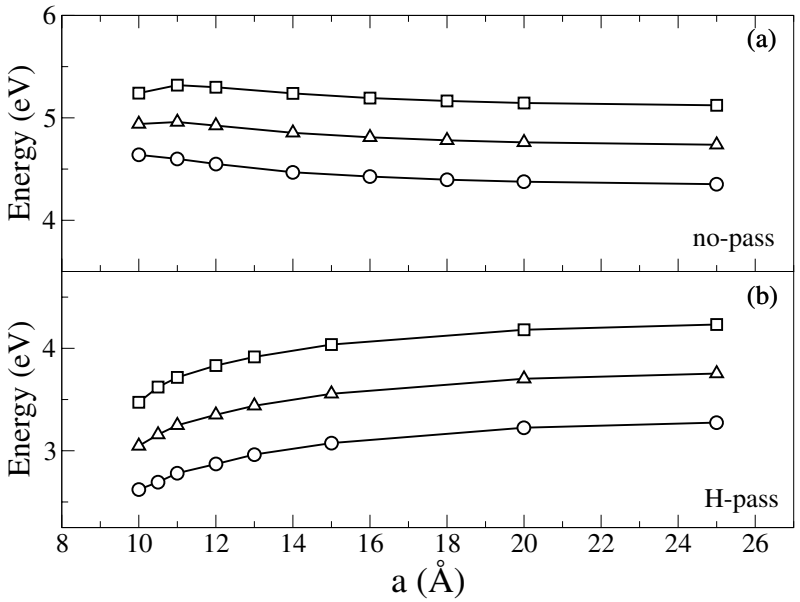

Figure 8. Ionization potential (squares), electron affinity (circles) and work function (triangles) for no-passivated (panel a) and H-passivated (panel b) (5,5) nanotube array, as a function of the array lattice parameter a. Lines are guides for the eyes.

edge shown by the Mulliken charge of Fig.2. This charge accumulation give rise to edge dipoles that with their orientation control the work function. When an array of nanotubes is formed, the surface density of dipole increases on reducing the array lattice spacing. We therefore have a work function that can either increase or decrease on reducing the lattice spacing, according to the dipole orientation. This is what Figs.2 and 8 show.

4. Conclusion

In this paper (5,5) and (7,0) H-passivated and no-passivated finite size carbon nanotubes have been studied using ab initio calculations. Taking together all the results we have obtained, it emerges that the EA and IP in finite carbon nanotubes are controlled by two concurrent effects. The first one is similar to a quantum confinement effect in that it gives a variation of both EA and IP with the nanotube length; the second is a purely electrostatic effect due to the formation of edge dipoles. In the case of a nanotube array, the third element that come into play is the array density through which the number of dipoles per surface area may be varied. Both EA and IP can either increase or decrease (with respect to the isolated nanotube) depending on the dipoles density and orientation. At least in principle, with a nanotechnological control on both the nanotube length and array density there are margins for tuning the electron affinity and the ionization potential. As a final remark, we would like to mention that in a recent paper [22] the work function of individual single wall carbon nanotubes have been measured with photoemission microscopy. Analyzing the data coming from a set nanotubes, the authors have been able to conclude that most of them have work functions whose differences are within 0.6 eV. Although it may be a fortuitous coincidence, the set of calculations presented in this work does give an overall work function variations in the range 0.5-0.6 eV.

Acknowledgments

This work have been done within the GINT collaboration (Gruppo INFN per le NanoTecnologie). Financial support from the Italian government through the COFIN-PRIN 2005 project is acknowledged. All the calculations have been performed at CINECA-"Progetti Supercalcolo 2007" and "Campus Computational Grid"-Università di Napoli "Federico II" advanced computing facilities.

References

[1] Anantram M P and Léonard F 2006 *Rep. Prog. Phys.* **69** 507 and references therein
[2] Shan B and Cho K 2005 *Phys. Rev. Lett.* **94** 236602
[3] Chen C W and Lee M H 2004 *Nanotechnology* **15** 480
[4] Su W S, Leung T C, Li B and Chan C T 2007 *Appl. Phys. Lett.* **90** 163103
[5] Agrawal B K, Agrawal S and Srivastava R 2003 *J. Phys.: Condens. Matter* **15** 6931

[6] Reich S, Thomsen C and Ordejón P 2002 *Phys. Rev.* B **65** 155411
[7] Wang Q, Setlur A, Lauerhaas J, Dai J, Seelig E and Chang R 1998 *Appl. Phys. Lett.* **72** 2912
[8] Li J, Papadopoulos C, Xu J and Moskovits M 1999 *Appl. Phys. Lett.* **75** 367
[9] Delley B 1990 *J. Chem. Phys.* **92** 508
[10] Delley B 2000 *J. Chem. Phys.* **113** 7756
[11] Baroni S, Corso A D, de Gironcoli S, Giannozzi P, Cavazzoni C, Ballabio G, Scandolo S, Chiarotti G, Focher P, Pasquarello A, Laasonen K, Trave A, Car R, Marzari N and Kokalj A http://www.pwscf.org
[12] Festa G, Cossi M, Barone V, Cantele G, Ninno D and Iadonisi G 2005 *J. Chem. Phys.* **122** 184714
[13] Perdew J P, Burke K and Ernzerhof M 1996 *Phys. Rev. Lett.* **77** 3865
[14] Andzelm J, King-Smith R D and Fitzgerald G 2001 *Chem. Phys. Lett.* **335** 321
[15] Nakada K, Fujita M, Dresselhaus G and Dresselhaus M 1996 *Phys. Rev.* B **54** 17954
[16] Gao R, Pan Z and Wang Z L 2001 *Appl. Phys. Lett.* **78** 1757
[17] Shiraishi M and Ata M 2001 *Carbon* **39** 1913
[18] Liu P, Wei Y, Jiang K, Sun Q, Zhang X, Fan S, Zhang S, Ning C and Deng J 2006 *Phys. Rev.* B **73** 235412
[19] Suzuki S, Bower C, Watanabe Y and Zhou O 2000 *Appl. Phys. Lett.* **76** 4007
[20] Lu D, Li Y, Rotkin S, Ravaioli U and Schulten K 2004 *Nano Lett.* **4** 2383
[21] Carlson A and Dumitrică; T 2007 *Nanotechnology* **18** 065706
[22] Saturo Suzuki, Yoshio Watanabe, Yoshikazu Homma, Shin-ya Fukuba, Stefan Heun, Andrea Locatelli 2004 *Appl. Phys. Lett.* **85** 127